# Excitation of coherent phonons in the one-dimensional Bi(114) surface

Leuenberger, D ; Yanagisawa, H ; Roth, S ; Dil, J H ; Wells, J H ; Hofmann, P ; Osterwalder, J ; Hengsberger, M

Abstract: We present time-resolved photoemission experiments from a peculiar bismuth surface, Bi(114). The strong one-dimensional character of this surface is reflected in the Fermi surface, which consists of spin-polarized straight lines. Our results show that the depletion of the surface state and the population of the bulk conduction band after the initial optical excitation persist for very long times. The disequilibrium within the hot electron gas along with strong electron-phonon coupling cause a displacive excitation of coherent phonons, which in turn are reflected in coherent modulations of the electronic states. Beside the well-known A1g bulk phonon mode at 2.76 THz, the time-resolved photoelectron spectra reveal a second mode at 0.72 THz which can be attributed to an optical surface phonon mode along the atomic rows of the Bi(114) surface.

DOI: https://doi.org/10.1103/PhysRevLett.110.136806

# Excitation of coherent phonons in the one-dimensional Bi(114) surface

D. Leuenberger,[1] H. Yanagisawa,[1,*] S. Roth,[1] J.H. Dil,[1,2] J.W. Wells,[3] P. Hofmann,[4] J. Osterwalder,[1] and M. Hengsberger[1]

[1]*Physics Institute, University of Zürich, Winterthurerstrasse 190, 8057 Zürich, Switzerland*
[2]*Swiss Light Source, Paul-Scherrer Institute, 5232 Villigen PSI, Switzerland*
[3]*Department of Physics, Norwegian University of Science and Technology, 7491 Trondheim, Norway*
[4]*Department of Physics and Astronomy and Interdisciplinary Nanoscience Center (iNANO), Aarhus University, 8000 Århus C, Denmark*

(Dated: February 25, 2013)

We present time-resolved photoemission experiments from a peculiar bismuth surface, Bi(114). The strong one-dimensional character of this surface is reflected in the Fermi surface, which consists of spin-polarized straight lines. Our results show that the depletion of the surface state and the population of the bulk conduction band after the initial optical excitation persist for very long times. The disequilibrium within the hot electron gas along with strong electron-phonon coupling cause a displacive excitation of coherent phonons, which in turn are reflected in coherent modulations of the electronic states. Beside the well-known $A_{1g}$ bulk phonon mode at 2.76 THz the time-resolved photoelectron spectra reveal a second mode at 0.72 THz which can be attributed to an optical surface phonon mode along the atomic rows of the Bi(114) surface.

Reduced dimensionality at solid surfaces results in unique characteristics of the electronic structure as compared to the bulk. In the extreme case of a recently discovered phase of solids, the topology of the bulk band structure demands the existence of topologically protected metallic states at the solid surface [1, 2]. Bismuth, a semi-metal, features metallic surface states on all surfaces studied so far, giving a strong enhancement of the metallic density of states (DOS) at the surface [3–6]. The degeneracy of surface states is lifted due to strong spin-orbit coupling in bismuth and the broken inversion symmetry at the surface (Rashba-effect) [6]. In particular, the strongly anisotropic (114)-surface was found to support a metallic and spin-split quasi-one-dimensional (1D) surface state [7]. The momenta $\mathbf{k}_F$ of the states at the Fermi energy $E_F$ form straight lines close to the $\overline{\Gamma}$-points of the surface reciprocal lattice and perpendicular to the direction $[1\bar{1}0]$ of the atomic rows. In such a topology, any low-energy perturbation providing the momentum required to connect two parallel sections of the Fermi surface, generates a strong electronic response. This leads to instabilities of the system, which may appear as charge- or spin-density waves, for instance [8]. Previously, such a charge-density wave (CDW) ground state was proposed for Bi(111) [9] based on the hexagonal shape of the Fermi contour of the electron pocket at $\overline{\Gamma}$. A combined photoemission and tunneling microscopy study, however, provided no evidence for a CDW [10]. Kim and co-workers argued that the states at opposite momenta carrying opposite spin, any scattering between these states requires spin-flip.

Thus, the situation on Bi(114) is particularly interesting: The Fermi surface topology renders the metallic surface states instable, and the distorted rhombohedral lattice makes it sensitive to displacive excitations of coherent optical phonons (DECP) [11–15]. Such coherent oscillations feed strong electronic modulations in space and time. Due to spin-orbit interaction, the spins of states at momenta $+\mathbf{k}_F$ and $-\mathbf{k}_F$ have anti-parallel orientation [7], what inhibits scattering between these states. The Bi(114) surface therefore offers the unique possibility to study the competing effects of spin-momentum locking, electron-phonon coupling, and Fermi surface topology in reduced dimensions.

The crystal was cleaned *in situ* by cycles of argon sputtering and annealing at 300 K [7]. We excite the sample with a linearly $p-$polarized infrared pump pulse ($h\nu_1 = 1.55$ eV) [16]. In the measurements shown here, the absorbed pump fluence was set to 0.57 mJ/cm$^2$, corresponding to an excitation density of $n \approx 0.34\%$ of the valence electron density [14]. The electronic structure was probed by two-photon photoemission ($2 \times h\nu_2 = 2{\times}3.1$ eV, $\Delta t_{probe} = 50$ fs), and the photoelectrons were detected using a hemispherical electron analyzer [17]. The combined energy resolution was about 50 meV, the angular resolution was $\pm 1°$. All measurements were performed at room temperature.

The Bi(114) surface consists of straight atomic rows running along $[1\bar{1}0]$, which are separated by 28 Å wide valleys [7], as shown in Fig. 1. The 1D spatial character is reflected in the electronic structure. The Fermi surface maps in Figs. 1(a) and (c) reveal straight lines parallel to $\overline{\Gamma Y}$, which were attributed to a spin-split 1D surface state [7]. All other features derive from bulk states. They disperse according to the bulk BZ and possess a defined symmetry only with respect to the remaining mirror plane $\{yz\}$. The surface state is localized perpendicular to the atomic chains and strongly dispersing along the chains ($\overline{\Gamma X}$). Energy spectra taken for momenta along $\overline{\Gamma X}$ reveal the surface state on top of Λ-shaped bulk bands, and with the band bottom at a binding energy of 100 meV, as shown in Figs. 1(b), (d), and (e). The agreement be-

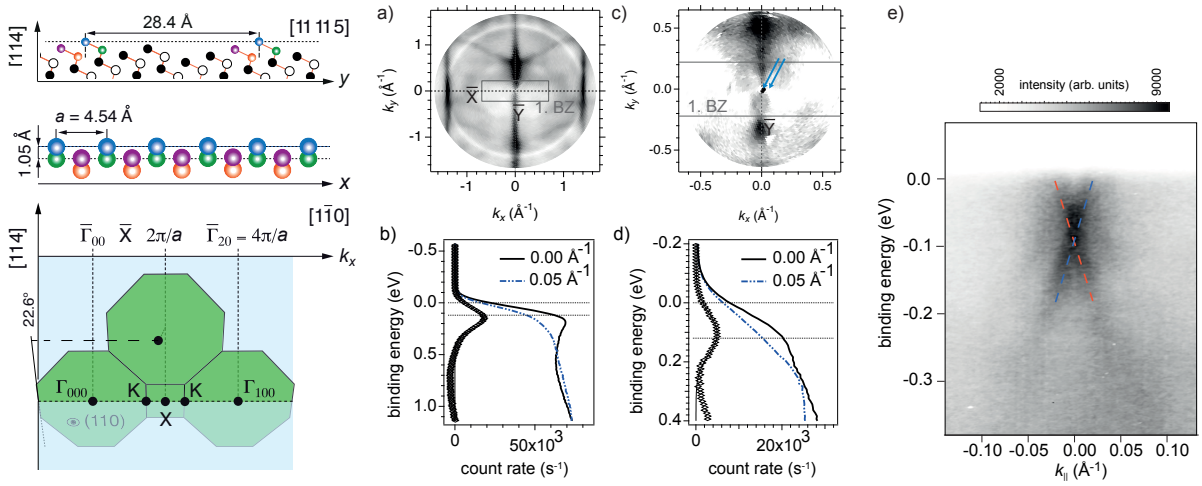


FIG. 1: (Colour online) Sketch of the atomic structure of Bi(114); atoms in the rows are colored; bottom: Brillouin zones for surface and bulk in the plane of the binary axis and the surface normal; the projection of the bulk $X$-point corresponds to the center of the second surface BZ $\Gamma_{10}$. The green shaded (110) plane is tilted out of the image plane. Panels (a)-(e): Photoemission data taken at the Fermi level with $h\nu = 21.2$ eV (a and b) and with $2 \times 3.1$ eV (c and d): (a) and (c) Fermi surfaces (black = high intensity). (b) and (d) Two selected spectra taken for momenta indicated by the blue arrows in (c); the black open diamonds in (b) and (d) show the difference between the two spectra, *i.e.* the surface state. (e) Band dispersion recorded using $h\nu = 21.2$ eV (spin-integrated). Dashed lines are guides to the eye, the color mimics spin polarisations.

tween one-photon photoemission and low-energy 2PPE data, shown in Figs. 1(a)-(b) and (c)-(d), respectively, ensures that the low-energy data contain no contribution from intermediate states in the unoccupied regime [18].

In Fig. 2, data are shown as function of time delay, taken close to normal emission ($k_x = k_F = 0.037$ Å$^{-1}$). Note that only the surface state contributes to the intensity at the Fermi level. At zero pump-probe delay, the bulk conduction band is populated with a transient hot electron population following absorption of the pump pulse. Possible momentum-conserving transitions along [114] are depicted in Fig. 2(a). The electrons excited into the conduction band relax by scattering and accumulate at the band bottom, where they appear as a broad feature in the spectra, Fig. 2(b).[20] The evolution of the hot electron distribution can be seen in the false color plots in Figs. 2(c) and (d). The thermalization and, eventually, the energy dissipation last over several picoseconds. In order to investigate the dynamics of the hot electron gas quantitatively, spectra and transients were fitted using Fermi-Dirac distributions and rate equations, respectively. The results are plotted in Fig. 3. The electronic temperature $T_{el}$ rises up to about 2000 K with a time constant of 260 fs. The time constant and the maximum temperature are in agreement with results of a previous study [21] and estimates based on the fluence [22], respectively. The initial rise is followed by a slow cooling of $T_{el}$ and energy dissipation from the electronic system to the lattice within about 5.9 ps.

The cooling of the electronic system is accompanied by a corresponding shift of the band bottom on the same timescales, as shown in Fig. 3(b): Ignoring at present the first spike-like increase of the energy position, the average peak position shifts by 60 meV towards lower energies within a few hundreds of femtoseconds and subsequently relaxes back on a picosecond timescale. Similar observations were made very recently on Bi(111): following absorption of an infrared pump pulse both, surface and bulk states shifted to lower energy [23]. The transient follows the electronic temperature like in our case. Since the origin could not be elucidated so far, we conjecture that the shift is caused by a charge redistribution due to the excitation of hot electrons.

The intensity cross correlation curves reveal two timescales $\tau_i$ and $\tau_{ii}$ depending on the electron energy, as can be seen in Figs. 3(c) and (d): The long decay time $\tau_{ii}$ for electrons from the conduction band bottom or below reflect thermally excited states for delays larger than 1.5 ps and, thereby, the evolution of $T_{el}$. The faster timescale $\tau_i$ for energies within the conduction band (about 0.6 eV and higher) is caused by comparably fast scattering within the conduction band, which dominates the decay of these states. The energy dependence corresponding to a power law with an exponent of $-1.5$ depends on details of the transient electronic distribution function [24]. A detailed discussion is beyond the scope of this paper.

The dynamics found here for Bi(114) strongly resemble those observed very recently in the topolocial insulator $Bi_2Se_3$ [25]: a fast intraband decay by electron-phonon scattering within the conduction band is followed by a much slower decay on a picosecond timescale for both the bulk conduction band and the metallic surface state. The second, long timescale is a consequence of the low scatter-

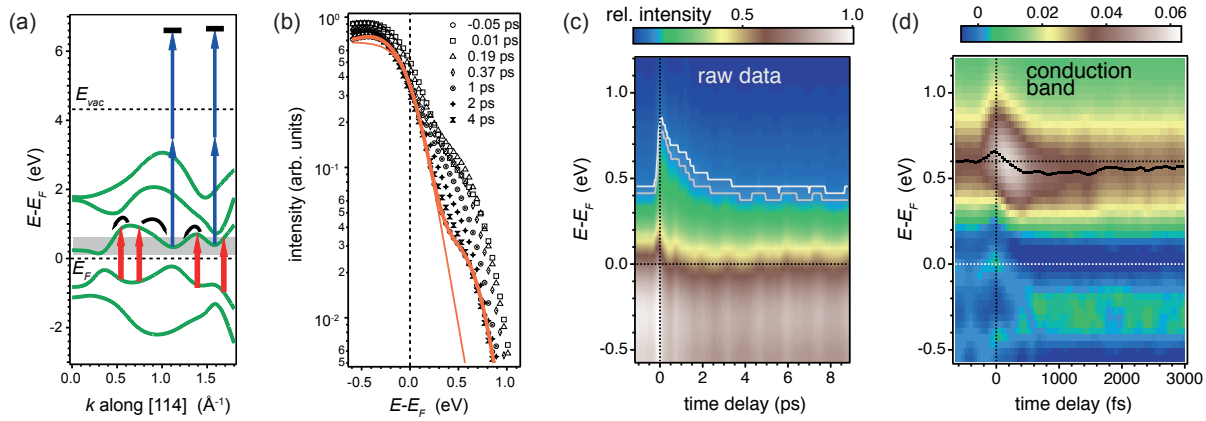


FIG. 2: (Color online) (a) Momentum conserving transitions from the 5th to the 6th valence band along [114], which can contribute to the hot electron population close to $\overline{\Gamma}$; energy bands (green lines) were calculated in a tight-binding scheme [19]; electrons are excited by 1.55 eV photons (red arrows) and accumulate in a minimum of the conduction band (grey shaded), where they are probed by 2PPE (blue arrows). (b) Spectra (symbols) taken close to $\overline{\Gamma}$ for various delays between -0.05 ps and 4 ps showing the signature of hot electrons above $E_F$. The thick (thin) orange line denotes an fit of two Gaussians multiplied with a Fermi-Dirac distribution (bare Fermi-Dirac distribution). (c) Plot of the intensity as function of energy and time delay. (d) Same data after subtraction of the Fermi-Dirac distribution for each individual delay. The black line follows the transient energy position of the conduction band.

ing probability due to the low DOS at $E_F$ in Bi and the energy difference between conduction band and surface state, which is large compared to typical phonon frequencies. Here, however, we find strong evidence for simultaneous emission of many quanta of particular phonon modes from the observation of intensity and energy modulations of the peaks, which can readily be recognized in Fig. 2(c).

In order to quantify these effects, intensity transients were recorded for the surface state and the conduction band. The data were normalized to those at negative delay times. Two selected transients are displayed for two different pump pulse durations in Fig. 4(a). The cosine-like modulations are assigned to excitations of coherent phonon modes. Such modes are known to modulate bulk electronic states, allowing them to be directly observed in photoemission spectra [26–29]: the excitation of many electronic transitions results in a displacement of the minimum of the free energy towards a crystal structure closer to the cubic lattice [14]. The atoms then start to perform damped oscillations around the new positions. This phenomenon is called coherent if the initial excitation occurs within a time shorter than half a phonon cycle. As a consequence, the electronic spectral weight and energy position follow the changing atomic positions. Given that the electronic response is faster than the time period of the phonon mode, the phase of the coherent phonon is directly imprinted in the spectra. The amplitude of the oscillations in binding energy (Fig. 3b) is of the order of 20 meV, which is in agreement with photoemission data taken recently from Bi(111) under comparable conditions and corresponds to an atomic displacement of about 1-

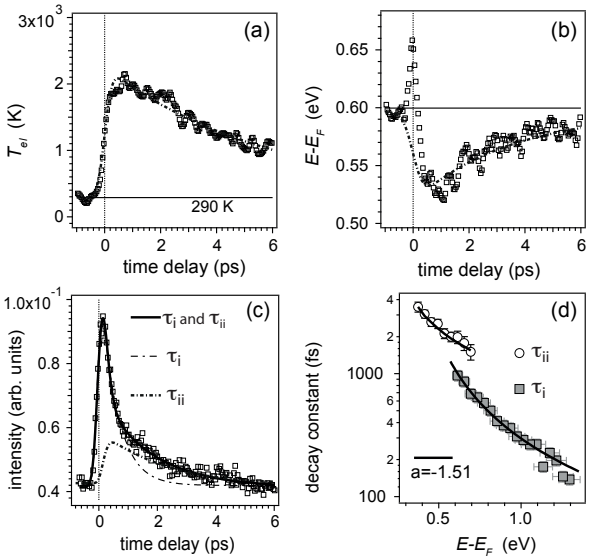


FIG. 3: (a) Electron temperature $T_{el}$ and (b) transient position of the conduction band as function of delay [Fig. 2(d)]. (c) Cross correlation curve obtained from the conduction band at 0.57 eV above $E_F$; the solid line corresponds to a double-exponential fit with two decay constants $\tau_i$ and $\tau_{ii}$; the dashed lines represent the two distinct contributions. (d) $\tau_{ii}$ and $\tau_i$ as obtained from the fits as function of energy above $E_F$. The line represents a power law fit $(E - E_F)^{-1.5}$.

2 pm [23].

The Fourier transform (FT) of the measured oscillations, displayed as top trace in Fig. 4(b) for a temporal pump pulse width $\Delta t_{pump}$ of 160 fs, reveals two dominant frequencies: The first frequency of 2.76(2) THz is close to

the softened longitudinal optical (LO) $A_{1g}$ mode, found at roughly 2.85 THz in numerous time-resolved experiments [11–15] at the Γ-point of the bulk BZ. The second frequency of 0.72(1) THz corresponds to an oscillation period of 1.39(1) ps. The observation of this mode can be explained by the peculiar band structure of Bi(114) as will be discussed below.

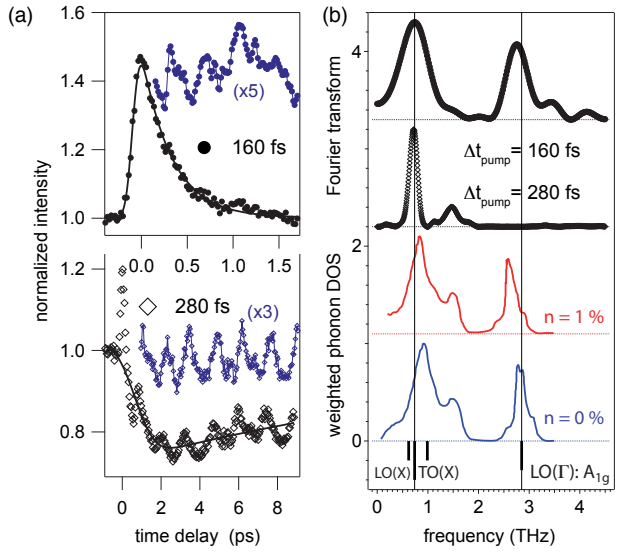


FIG. 4: (Color online) (a) Transient photoemission intensity at the conduction band for a *short* pump pulse (top panel) and at $E_F$ for a long pump pulse (bottom panel) as function of time delay. The data are shown as raw data and after subtraction (blue) of fitted rate equations (solid lines) in order to highlight the oscillations. (b) Fourier transform of the measured intensity cross correlations for the two different temporal pump pulse durations (solid symbols: $\Delta t_{pump} = 160$ fs; open symbols: $\Delta t_{pump} = 280$ fs). Bottom: calculated phonon DOS $F(\omega)d\omega$ (Ref. 30) weighted by $\omega^{-1}$ for the ground state (blue) and for n = 1% excited valence electrons (red).

Assuming the electron-phonon coupling strength to scale with inverse phonon frequency, the FT may be compared to $F(\omega)d\omega/\omega$ [31], where $F(\omega)d\omega$ denotes the phonon DOS in the frequency interval $[\omega, \omega + d\omega]$. This function, which was calculated using the phonon DOS for two different electron excitation densities [30], is displayed in Fig. 4(b). Two van Hove singularities dominate these spectra, one around 2.8 THz for the optical modes at Γ, and the second at about 0.7 THz corresponding to modes at the zone boundary along $\Gamma KX$ of the bulk BZ.

We focus on the low-frequency mode at 0.72 THz. The excitation of this mode can either be the result of a strong decay channel of the high-frequency $A_{1g}$ mode or else result itself from a coherent electronic excitation. In order to discriminate between both excitation pathways, the pump pulse duration was increased to $\Delta t = 280$ fs by introducing linear chirp by means of a grating compressor. Since half the temporal period of the $A_{1g}$ mode corresponds to about $T_{A1g}/2 \approx 180$ fs, the condition $\Delta t < T_{A1g}/2$ for coherent phonon excitation is no longer fulfilled. As a consequence, the $A_{1g}$ mode is suppressed [see Fig. 4]. The low-frequency mode at 0.72 THz, on the other hand, persists giving evidence for a coherent excitation of this mode via electronic transitions.

The fact that this mode is directly excited can be explained by the low dimensionality of the surface [8]. The strongly enhanced susceptibility of surface state electrons to excitations with momenta along the atomic chains increases the coupling significantly. Indeed, the strong phonon DOS around 0.7 THz in Fig. 4(b) is due to van Hove singularities in three branches midway between two adjacent reciprocal lattice points along $\Gamma KX$. This corresponds to a standing wave along the binary axis $[1\bar{1}0]$, *i.e.* along the atomic chains. Since the distance $\Gamma KX$ in reciprocal space corresponds to a reciprocal lattice vector of the surface along the rows, the mode is equivalent to an optical surface phonon with momentum $q = 0$. The character of the bulk branches is acoustic in the long wavelength limit and changes to two transverse $TO(X)$ and one longitudinal optical $LO(X)$ branches at the border of the BZ[30]. Previously, a weak signal at 0.68 THz was reported from reflectivity measurements on Bi films [32] and interpreted as transverse-acoustic mode $X$, in agreement with our interpretation of the Fourier spectra. Surprisingly and in contrast to the previous study on Bi(111) [23], the surface states are strongly modulated indicating that we are dealing here with a phonon mode in the chains of Bi(114).

Eventually, the following picture emerges: due to the 1D character of the surface, the electronic response function to perturbations diverges for momenta connecting large portions of the Fermi surfaces. A phonon modulating the atomic structure along the rows generates a large electronic response, which manifests itself as a modulation in the photoelectron spectra. A suitable phonon mode is given by an optical bulk mode with correct frequency and momentum along $[1\bar{1}0]$. On Bi(114), adjacent Fermi surfaces have opposite spin polarization owing to strong spin-orbit splitting lifting the spin degeneracy at the surface. This inhibits a nesting of the Fermi surfaces for small momentum transfer and protects the metallic states against a charge-density wave transition [10, 33].

In conclusion, the transient occupation of the bulk conduction band of Bi leads to the excitation of two coherent optical phonon modes in Bi(114). Beside the $A_{1g}$ bulk phonon a second mode at 0.72 THz is found to strongly modulate the surface electronic states on a picosecond time scale. This mode could be identified as an electronically induced DECP of an optical surface phonon mode along the atomic rows of Bi(114).

We gratefully acknowledge J.I. Pascual and A. Strozecka for valuable discussions. This work was supported by the Swiss National Science Foundation and by the Swiss National Science Foundation through the National Center of Competence in Research MUST.

* Present address: Institute of Quantum Electronics, Swiss Federal Institute of Technology, Wolfgang-Pauli-Strasse 16, 8093 Zürich, Switzerland


[1] D. Hsieh, D. Qian, L. Wray, Y. Xia, Y. S. Hor, R. J. Cava, and M. Z. Hasan, Nature **452**, 970 (2008).

[2] M. Z. Hasan and C. L. Kane, Rev. Mod. Phys. **82**, 3045 (2010).

[3] M. Hengsberger, P. Segovia, M. Garnier, D. Purdie, and Y. Baer, Eur. Phys. J. B **17**, 603 (2000).

[4] S. Agergaard, C. Sondergaard, H. Li, M. B. Nielsen, S. V. Hoffmann, Z. Li, and Ph. Hofmann, New J. of Phys. **3**, 15.1 (2001).

[5] C. R. Ast and H. Höchst, Phys. Rev. Lett. **87**, 177602 (2001).

[6] Ph. Hofmann, Progress in Surface Science 81 **81**, 191 (2006).

[7] J. W. Wells, J. H. Dil, F. Meier, J. Lobo-Checa, V. N. Petrov, J. Osterwalder, M. M. Ugeda, I. Fernandez-Torrente, J. I. Pascual, E. D. L. Rienks, et al., Phys. Rev. Lett. **102**, 096802 (2009).

[8] G. Grüner, *Density Waves in Solids*, vol. 89 of *Frontiers in Physics* (Addison Wesley Publishing, Reading, Menlo Park, New York, 1994).

[9] C. R. Ast and H. Höchst, Phys. Rev. Lett. **90**, 016403 (2003).

[10] T. K. Kim, J. Wells, C. Kirkegaard, Z. Li, S. V. Hoffmann, J. E. Gayone, I. Fernandez-Torrente, P. Häberle, J. I. Pascual, K. T. Moore, et al., Phys. Rev. B **72**, 085440 (2005).

[11] T. K. Cheng, S. D. Brorson, A. S. Kazeroonian, J. S. Moodera, G. Dresselhaus, M. S. Dresselhaus, and E. P. Ippen, Appl. Phys. Lett. **57**, 1004 (1990).

[12] M. Hase, K. Mizoguchi, H. Harima, S. Nakashima, M. Tani, K. Sakai, and M. Hangyo, Appl. Phys. Lett. **100**, 2474 (1996).

[13] K. Sokolowski-Tinten, C. Blome, J. Blums, A. Cavalleri, C. Dietrich, A. Tarasevitch, I. Uschmann, E. Förster, M. Kammler, M. H. von Hoegen, et al., Nature **422**, 287 (2003).

[14] D. M. Fritz, D. A. Reis, B. Adams, R. A. Akre, J. Arthur, C. Blome, P. H. Bucksbaum, A. L. Cavalieri, S. Engemann, S. Fahy, et al., Science **315**, 633 (2007).

[15] S. L. Johnson, P. Beaud, E. Vorobeva, C. J. Milne, E. D. Murray, S. Fahy, and G. Ingold, Phys. Rev. Lett. **102**, 175503 (2009).

[16] D. Leuenberger, H. Yanagisawa, S. Roth, J. Osterwalder, and M. Hengsberger, Phys. Rev. B **84**, 125107 (2011).

[17] T. Greber, O. Raetzo, T. Kreutz, P. Schwaller, W. Deichmann, E. Wetli, and J. Osterwalder, Rev. Sci. Instrum. **68**, 4549 (1997).

[18] M. Hengsberger, F. Baumberger, H. J. Neff, T. Greber, and J. Osterwalder, Phys. Rev. B **77**, 085425 (2008).

[19] Y. Liu and R. E. Allen, Phys. Rev. B **52**, 1566 (1995).

[20] Note that the global bulk conduction band minimum is below the Fermi energy. We refer to the band bottom here as being the energy minimum of the bulk conduction band along [114], as observed in the photoemission spectra for this geometry.

[21] S. L. Johnson, P. Beaud, C. J. Milne, F. S. Krasniqi, E. S. Zijlstra, M. E. Garcia, M. Kaiser, D. Grolimund, R. Abela, and G. Ingold, Phys. Rev. Lett. **100**, 155501 (2008).

[22] D. Boschetto, T. Garl, and A. Rousse, Journal of Modern Optics **57** (2010).

[23] E. Papalazarou, J. Faure, J. Mauchain, M. Marsi, A. Taleb-Ibrahimi, I. Reshetnyak, A. van Roekeghem, I. Timrov, N. Vast, B. Arnaud, et al., Phys. Rev. Lett. **108**, 256808 (2012).

[24] B. Rethfeld, A. Kaiser, M. Vicanek, and G. Simon, Phys. Rev. B **65**, 214303 (2002).

[25] J. A. Sobota, S. Yang, J. G. Analytis, Y. L. Chen, I. R. Fisher, P. S. Kirchmann, and Z. X. Shen, Phys. Rev. Lett. **108**, 117403 (2012).

[26] L. Perfetti, P. A. Loukakos, M. Lisowski, U. Bovensiepen, H. Berger, S. Biermann, P. S. Cornaglia, A. Georges, and M. Wolf, Phys. Rev. Lett. **97**, 067402 (2006).

[27] L. Perfetti, P. A. Loukakos, M. Lisowski, U. Bovensiepen, M. Wolf, H. Berger, S. Biermann, and A. Georges, New J. Phys. **10**, 053019 (2008).

[28] F. Schmitt, P. S. Kirchmann, U. Bovensiepen, R. G. Moore, L. Rettig, M. Krenz, J.-H. Chu, N. Ru, L. Perfetti, D. H. Lu, et al., Science **321**, 1649 (2008).

[29] L. Rettig, P. S. Kirchmann, and U. Bovensiepen, New J. Phys. **14**, 023047 (2012).

[30] E. D. Murray, S. Fahy, D. Prendergast, T. Ogitsu, D. M. Fritz, and D. A. Reis, Phys. Rev. B **75**, 184301 (2007).

[31] P. B. Allen, Phys. Rev. Lett. **59**, 1460 (1987).

[32] A. Wu and X. Xu, Appl. Surf. Sci. **253**, 6301 (2007).

[33] C. Tegenkamp, D. Lükermann, H. Pfnür, B. Slomski, G. Landolt, and J. H. Dil, Phys. Rev. Lett. **109**, 266401 (2012).